IEEE Access
Multidisciplinary : Rapid Review : Open Access Journal

Received December 27, 2020, accepted January 7, 2021, date of publication January 19, 2021, date of current version February 3, 2021.

Digital Object Identifier 10.1109/ACCESS.2021.3052465

An Adaptive-Tunable-Based Hybrid RBF Network for EGTM Prediction

YUAN LIU[1], XIANPING ZENG[2], YANYUN TIAN[1], YISHOU WANG[2], AND HANLIN SHENG[3], (Member, IEEE)
[1]AECC Hunan Aviation Powerplant Research Institute, Zhuzhou 412000, China
[2]School of Aerospace Engineering, Xiamen University, Xiamen 361000, China
[3]College of Energy and Power Engineering, Nanjing University of Aeronautics and Astronautics, Nanjing 210016, China

Corresponding authors: Xianping Zeng (mrszxp@163.com) and Hanlin Sheng (dreamshl@qq.com)

This work was supported in part by the National Natural Science Foundation of China under Grant 51975494, and in part by the Fundamental Research Funds for the Central Universities under Grant 20720180120.

ABSTRACT Aero-engine exhaust gas temperature margin (EGTM) is one of the main indexes of engine replacement; however, the application of existing methods in EGTM forecasting is restricted because of the limited prediction accuracy and many non-linearities. In this study, an adaptive-tunable-based hybrid radial basis function (RBF) network is proposed to improve the prediction accuracy of aero-engine EGTM. Firstly, a hybrid RBF network consisting of a RBF network and a linear regression model is built as a fundamental EGTM predictive algorithm. Secondly, to increase the network's adaptation capabilities, the structural parameters of the proposed network are adaptively modulated by Brownian motion modeling and particle filter without physics-based models. Finally, multiple sets of EGTM data from a certain type aero-engines in an airline company is selected for engine removal time prediction. Experiment results demonstrate that the proposed adaptive-tunable-based hybrid RBF network with a high prediction accuracy, and can reflect the characteristics of EGTM well and truly, which can capture the dynamic nature of EGTM in time during the forecasting process.

INDEX TERMS Aero-engine, exhaust gas temperature margin prediction, hybrid RBF network, Brownian motion, particle filter.

I. INTRODUCTION

The predictive replacement of aero-engine is an important means to improve the economics and safety of the entire fleet. The decrease of exhaust gas temperature margin (EGTM) in the take-off phase of an aero-engine is one of the main reasons for engine replacement [1], [2], that is, to replace engine when EGTM decays to a given threshold [3]. Therefore, it is possible to evaluate the reliability of the engine and predict the engine replacement time by analyzing the declining trend of the take-off EGTM. Unless otherwise specified, the EGTM mentioned below refers to the EGTM in the take-off phase.

The aero-engine is a complex nonlinear system and EGTM presents complex and variability as the engine's working state changes [4]. A lot of researches on EGTM prediction [5]–[15] had been conducted by many scholars. Generally, the modeling methods of the degradation statistical model can be divided: methods based on data-driven, methods based on product failure mechanisms, and methods based on the combination of data-driven and failure mechanisms [5], [6]. The method based on data-driven is to analyze and process the real-time monitoring data during the operation of the engine without the need to establish an accurate mathematical model of the engine, which is simple and practical, has been widely used. For example, Kumar *et al.* [7] applied autoregressive and moving average techniques to predict EGTM of aero-engine. Ren [8] and Gao and Wang [9] adopted Kalman filter approach to monitor an aero-engine health and condition by building prediction models of the EGTM and other key performance parameters, which well addressed the randomness problem of performance parameter variation. These methods are carried out under the assumption of linear model, whereas in general, the performance parameter variation of aero-engine is nonlinear. Besides, neural networks have gained popularity in the research of EGTM prediction due to the good nonlinear mapping capabilities. Ilbas and Turkmen [10]

The associate editor coordinating the review of this manuscript and approving it for publication was Camelia Delcea.

had considered artificial neural networks to predict the EGT of the CFM56-7B engine; while Iman *et al.* [11] combined polynomial regression and neural network methods to predict and evaluate EGT of the aero-engine; Rai *et al.* [12] proposed an adaptive neuro-fuzzy inference system to establish a prediction model of EGTM of the engine, brake specific energy consumption and other performance parameters; literature [13] and [14] adopted long and short term memory network(LSTM) to build aero-engine EGTM prediction model, using the time-based back-propagation algorithm for forwarding calculation and error back-propagation to update and train the prediction model to realize the prediction of EGTM data at the future time; Pi *et al.* [15] had applied an improved fruit fly algorithm to optimize the generalized regression neural network (GRNN), and used the optimized GRNN to predict the EGT of the aero-engine. The predicted values using these models agreed well with measurements data; however, the nonlinear mapping capabilities of most neural networks are related to adjustment parameters, such as the network's nuclear parameters and penalty parameters, the number of neurons in some neural networks, and the input matrix settings, which will have a greater impact on the prediction model. What's more, the degraded state of the engine will change with changes in operating conditions, and the engine dispatch prediction method based on a fixed structure can't capture the dynamic nature and pattern of the time series in time.

In view of aforementioned issues, this work focuses on EGTM forecasting by adopting a novel surrogate model based on an adaptive tunable hybrid neural network, which can adaptively modulate the structural parameters of the model. Considering the Radial Basis Function (RBF) neural network with the preponderance of strong nonlinear fitting ability, simple structure,.etc. For example, Mao *et al.* [16] used back-propagation(BP), Elman network, RBF and generalized regression neural network (GRNN) to predict the performance of the target engine, according to the results of the four network assessments, RBF with the best prediction effect. The RBF is very precise and practical method to perform the prediction and model nonlinear phenomena of engine performance. Accordingly, based on RBF neural network, this study proposes a hybrid RBF neural network prediction model with a variable online structure. The structure and parameters of the hybrid RBF neural network change dynamically, which is as new samples are continuously added, the network structure and parameters can be adjusted dynamically to capture the dynamic nature of the time series in time. Firstly, a hybrid RBF network consisting of a RBF network and a linear regression model is built as a fundamental EGTM predictive algorithm. And then the structural parameters of the proposed network are adaptively modulated by Brownian motion modeling and particle filter. Finally, the EGTM data of multiple engines of a certain type of an aviation company is selected for real-time distribution prediction to verify the feasibility of the method in the prediction of aero-engine performance parameters.

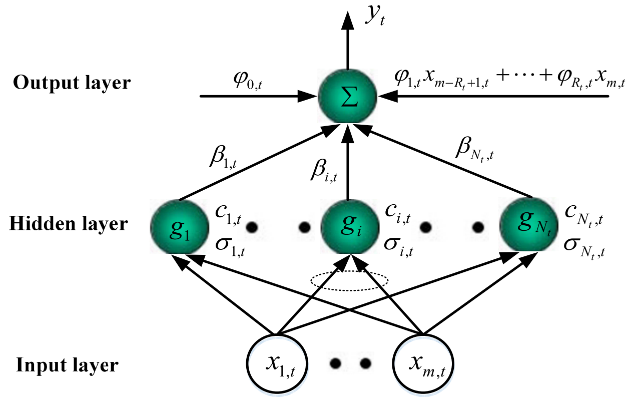

FIGURE 1. Hybrid RBF network model.

The remainder of this article is arranged as follows: Section II presents a detailed description of the adaptive tunable hybrid RBF network prediction methodology. Experimental investigation and comparison are given in Section III. Section IV summarizes the conclusions.

II. HYBRID RBF NEURAL NETWORK METHOD BASED ON ONLINE VARIABLE STRUCTURE

A. HYBRID RBF NEURAL NETWORK

The characteristics of non-linearity, atypicality, and non-equivalence of gas path performance changes during aero-engine operation make the EGTM data analysis inherently complex. And the hybrid RBF model composed of a single RBF network and linear regression term, not only with the advantage of the RBF network in function approximation, but also possess the preponderance of the autoregressive model in linear characteristics [17]. Hence, the hybrid RBF model can be better used to solve the EGTM prediction problem.

Suppose a training sample set $\{(\boldsymbol{X_t}, y_t)\}$ consisting of a group of data D, where c is the input vector, m represents the feature dimension of the input; y_t is the corresponding EGTM value.

As shown in Figure 1, a hybrid RBF network model consisting of $N_t(N_t < D)$ hidden layer nodes and linear regression terms are initially constructed, and its mathematical expression is:

$$y_t = \sum_{s=1}^{N_t} \beta_{s,t} g\left(\left\|X_t - c_{s,t}\right\|\right) + \varphi_{0,t} + \mathbf{\Phi}_t^T \bar{X}_t, \quad 1 \le t \le D \tag{1}$$

wherein, $\|\cdot\|$ is the distance measurement value, usually Euclidean norm; $g(\cdot)$ is the radial basis function, where a Gaussian radial basis function of form $g(x) = \exp(-x^2/2\sigma_{s,t}^2)$ is selected, wherein $\sigma_{s,t}$ is the variance (width) parameter of the network, and $s = 1,2,\cdots,N_t$. $\beta_{s,t}$ represents the connection weight between the s hidden layer node and the output node, which is the center of the s hidden layer node $c_{s,t} = [c_{s,1,t}, c_{s,2,t}, \cdots, c_{s,m,t}]^T$ in the RBF network. $\varphi_{0,t}$ and $\mathbf{\Phi}_t = [\varphi_{1,t}, \cdots, \varphi_{R_t,t}]^T$ represent the linear regression coefficient, where R_t is the order of the autoregressive model, $\bar{\boldsymbol{X}}_t = [x_{m-R_t+1,t}, \cdots, x_{m,t}]^T$ at this time.

simplify (1) into matrix form:

$$y_t = H_t \beta_t \tag{2}$$

where, $H_t = [1, x_{m-R_t+1}, \cdots, x_m, g(X_t, c_{1,t}, \sigma_{1,t}), \cdots, g(X_t, c_{N_t,t}, \sigma_{N_t,t})]$, $\beta_t = [\varphi_{0,t}, \varphi_{1,t}, \cdots, \varphi_{R_t,t}, \beta_{1,t}, \cdots, \beta_{N_t,t}]^T$.

Because of the problem that the neural network structure is too large or too small, this paper uses particle filtering to dynamically adjust the hybrid RBF network, that is, as new samples are continuously added, the network structure parameters $N_t, R_t, c_{s,t}, \sigma_{s,t}, \beta_t$ are dynamically adjusted online to capture the dynamics nature's change of aero-engine EGTM in time.

B. ONLINE VARIABLE STRUCTURE HYBRID RBF BASED ON PARTICLE FILTER PREDICTOR

The particle filter predictor is based on the Monte Carlo method [18], which mainly includes the steps of state transition, structural parameter update and online prediction.

1) STATE TRANSFER EQUATION

The Brownian with drift and scale parameters are particularly suitable for modeling the dynamic behavior of equipment aging, so it is widely used in the related fields of equipment remaining life prediction [19]. In this study, the structural parameters The N_t and R_t are respectively evolved by random walks according to a certain probability distribution (Brownian motion).

Let B_t represents the parameters at time t, the parametric transfer equation based on Brownian motion can be expressed as:

$$K_t = K_{t-1} + \lambda \int_{t-1}^{t} \kappa(\tau, \theta) d\tau + \sigma_B B_{t-(t-1)} + v_t \tag{3}$$

wherein, λ is the drift coefficient, σ_B is the scale coefficient. B_t is a random process subject to Brownian motion, and satisfies $B_{t-(t-1)} = \varepsilon_t \sqrt{\Delta t}$ in the time increment Δt, ε_t is a standard normal random process. v_t is Gaussian white noise with a mean value of 0 and a variance of Q_v. $\kappa(\tau, \theta)$ is the function of θ, which can be either a linear function or a nonlinear function. In this study, let $\kappa(\tau, \theta) = 1$, so Equation (3) can be simplified to:

$$K_t = K_{t-1} + \lambda \Delta t + \sigma_B \varepsilon_t \sqrt{\Delta t} + v_t \tag{4}$$

Let the network structure parameters N_t, R_t time increment $\Delta t = 1$, and let the structural parameter $c_{s,t}, \sigma_{s,t}, \beta_t$ add a random Gaussian disturbance term to evolve based on the previous moment. Therefore, the state transfer equation of the online structure variable RBF network prediction model is as follows:

$$\begin{cases} N_t = round(N_{t-1} + \lambda_N + \sigma_{BN} \varepsilon_{N,t} + v_{N,t}) \\ R_t = round(R_{t-1} + \lambda_R + \sigma_{BR} \varepsilon_{R,t} + v_{R,t}) \\ c_{s,t} = c_{s,t-1} + \varepsilon_c, \quad s = 1, 2, \cdots, N_t \\ \sigma_{s,t} = \sigma_{s,t-1} + \varepsilon_\sigma, \quad s = 1, 2, \cdots, N_t \\ \beta_t = \beta_{t-1} + \varepsilon_\beta \end{cases} \tag{5}$$

wherein, $round(\cdot)$ means rounding, and assuming $\varepsilon_\sigma \sim N(0, \delta_\sigma^2 I_{N_t \times N_t})$, $\varepsilon_c \sim N(0, \delta_c^2 I_{(N_t*m)\times(N_t*m)})$, $\varepsilon_\beta \sim N(0, \delta_\beta^2 I_{(N_t+R_t+1)\times(N_t+R_t+1)})$, where m represents the featural dimension of the input, and $\delta_c^2, \delta_\sigma^2, \delta_\beta^2$ is all constant, $I_{(N_t*m)\times(N_t*m)}, I_{N_t\times N_t}, I_{(N_t+R_t+1)\times(N_t+R_t+1)}$ is the unity matrix.

2) STRUCTURAL PARAMETER UPDATE

The changes of the dimensionality of parameters $c_{s,t}, \sigma_{s,t}, \beta_t$ that are caused by the changes of the structural parameters N_t and R_t, which in turn causes H_t, β_t to change, can be seen from Equation (1)-(5).

To display the parameter changes intuitively, H_{t-1}, β_{t-1} at time $t-1$ in Equation (2) are decomposed as follows:

$$\begin{cases} H_{t-1} = [H_{t-1,1}, H_{t-1,2}, H_{t-1,3}] \\ H_{t-1,1} = 1, H_{t-1,2} = [x_{m-R_{t-1}+1}, \cdots, x_m] \\ H_{t-1,3} = [g(X_{t-1}, c_{1,t-1}, \sigma_{1,t-1}), \cdots, \\ \qquad g(X_{t-1}, c_{N_{t-1},t-1}, \sigma_{N_{t-1},t-1})] \\ \beta_{t-1} = [\beta_{t-1,1}, \beta_{t-1,2}, \beta_{t-1,3}]^T \\ \beta_{t-1,1} = \varphi_{0,t-1}, \beta_{t-1,2} = [\varphi_{1,t-1}, \cdots, \varphi_{R_{t-1},t-1}] \\ \beta_{t-1,3} = [\beta_{1,t-1}, \cdots, \beta_{N_{t-1},t-1}] \end{cases} \tag{6}$$

3) IMPACT OF N_t CHANGE ON MODEL PARAMETERS

In this study first adjusts network parameters for N_t changes. N_t has only the following three possible variations: (1) $N_t = N_{t-1}$; (2) $N_t = N_{t-1} + M_1$ $(M_1 > 0)$; (3) $N_t = N_{t-1} - M_2$ $(0 < M_2 < N_{t-1})$. Where $M_1, M_2 \in Z$ and Z represent integers.

For case (1), the parameters do not need to be adjusted.

For case (2), the parameters H_t, β_t are adjusted as follows:

$$\begin{cases} H_{t,1} = H_{t-1,1}, H_{t,2} = H_{t-1,2} \\ H_{t,3} = [H_{t-1,3}, g(X_t, c_{N_{t-1}+1,t}, \sigma_{N_{t-1}+1,t}), \cdots, \\ g(X_t, c_{N_{t-1}+M_1,t}, \sigma_{N_{t-1}+M_1,t})] \\ \beta_{t,1} = \beta_{t-1,1}, \beta_{t,2} = \beta_{t-1,2} \\ \beta_{t,3} = [\beta_{t-1,3}, \beta_{N_{t-1}+1,t}, \cdots, \beta_{N_{t-1}+M_1,t}] \end{cases} \tag{7}$$

where, $c_{N_{t-1}+i,t} = X_t + \varepsilon_i, \boldsymbol{X}_t = [x_{1,t}, x_{2,t}, \cdots, x_{m,t}]^T$ (m represents the input feature dimension), ε_i is the random Gaussian disturbance term; $\sigma_{N_{t-1}+i,t}, \beta_{N_{t-1}+i,t}$ is the random number, and $i = 1, 2, \cdots, M_1$.

For case (3), firstly, the hidden layer neurons are sorted by using the multi-response sparse regression algorithm [20]; secondly, the position before sorting corresponding to the neuron with the smaller error M_2 is recorded; finally, the recorded neurons are cut out related parameters corresponding to neurons. Assuming that the corresponding positions of the deleted neurons are respectively

$th_1, th_2, \cdots, th_{M_2}$, and $1 \le th_1 < th_2 < \cdots < th_{M_2} \le N_{t-1}$. The parameters H_t, β_t are adjusted as follows:

$$\begin{cases} H_{t,1} = H_{t-1,1}, H_{t,2} = H_{t-1,2} \\ H_{t,3} = [g(X_t, c_{1,t}, \sigma_{1,t}), \cdots, g(X_t, c_{th_1-1,t}, \sigma_{th_1-1,t}), \\ g(X_t, c_{th_1+1,t}, \sigma_{th_1+1,t}), \cdots, g(X_t, c_{th_{M_2}-1,t}, \sigma_{th_{M_2}-1,t}), \\ g(X_t, c_{th_{M_2}+1,t}, \sigma_{th_{M_2}+1,t}), \cdots, g(X_t, c_{N_{t-1},t}, \sigma_{N_{t-1},t})] \\ \beta_{t,1} = \beta_{t-1,1}, \beta_{t,2} = \beta_{t-1,2} \\ \beta_{t,3} = [\beta_{1,t}, \cdots, \beta_{th_1-1,t}, \beta_{th_1+1,t}, \\ \qquad \cdots, \beta_{th_{M_2}-1,t}, \beta_{th_{M_2}+1,t}, \cdots, \beta_{N_{t-1},t}] \end{cases} \tag{8}$$

4) THE INFLUENCE OF R_t CHANGE ON MODEL PARAMETERS

After the model structure adjustment which is caused by the N_t change, the model parameters after the R_t change are adjusted.

R_t also has only the following three possible variations: (1)$R_t = R_{t-1}$; (2)$R_t = R_{t-1} + M_3$ ($M_3 > 0$ & $R_t \le m$); (3) $R_t = R_{t-1} - M_4$ ($0 < M_4 < R_{t-1}$). Where $M_3, M_4 \in Z$, Z represents an integer.

For case (1), the parameters do not need to be adjusted.

For case (2), the parameters are adjusted as follows:

$$\begin{cases} H_{t,1}^{(2)} = H_{t,1}^{(1)}, H_{t,3}^{(2)} = H_{t,3}^{(1)} \\ H_{t,2}^{(2)} = [x_{m-(R_{t-1}+M_3-1)}, x_{m-(R_{t-1}+M_3-2)}, \\ \qquad \cdots, x_{m-R_{t-1}}, H_{t,2}^{(1)}] \\ \beta_{t,1}^{(2)} = \beta_{t,1}^{(1)}, \beta_{t,3}^{(2)} = \beta_{t,3}^{(1)} \\ \beta_{t,2}^{(2)} = [\varphi'_{1,t}, \cdots, \varphi'_{M_3,t}, \beta_{t,2}^{(1)}] \end{cases} \tag{9}$$

wherein, $(\cdot)^{(2)}$, $(\cdot)^{(1)}$ respectively indicate the parameters after adjustment and before adjustment. $\varphi'_{1,t}, \cdots, \varphi'_{M_3,t}$ is a random number.

For case (3), the parameters are adjusted as follows:

$$\begin{cases} H_{t,1}^{(2)} = H_{t,1}^{(1)}, H_{t,3}^{(2)} = H_{t,3}^{(1)} \\ H_{t,2}^{(2)} = [x_{m-(R_{t-1}-M_4-1)}, x_{m-(R_{t-1}-M_4-2)}, \\ \qquad \cdots, x_{m-1}, x_m] \\ \beta_{t,1}^{(2)} = \beta_{t,1}^{(1)}, \beta_{t,3}^{(2)} = \beta_{t,3}^{(1)} \\ \beta_{t,2}^{(2)} = [\varphi_{R_{t-1}-(R_{t-1}-M_4-1)}, \\ \qquad \varphi_{R_{t-1}-(R_{t-1}-M_4-2)}, \cdots, \varphi_{R_{t-1}-1}, \varphi_{R_{t-1}}] \end{cases} \tag{10}$$

5) OVERALL FORECASTING PROCESS

The flowchart of the proposed approach can be seen in Figure 2. For significantly restricting the search space of the structural parameters of the network, a set of initial parameters $\Omega_0 = \{N_0, R_0, c_0, \sigma_0, \beta_0\}$ are obtained by pre-training the hybrid RBF network. And then the structural parameters of the hybrid network are adaptively modulated by Brownian motion modeling and particle filter predictor. The pseudo code of the detailed process is presented in Algorithm1.

First, a set of initial parameters can be obtained by using the hybrid RBF network: $\Omega_0 = \{N_0, R_0, c_0, \sigma_0, \beta_0\}$, where $c_0 = \{c_{s,0} | c_{s,0} = \{c_{s,i,0} i = 1, 2, \cdots, m\}$, $\sigma_0 = \{\sigma_{s,0}\}$, $s = 1, 2, \cdots, N_0$; $\beta_0 = [\varphi_{0,0}, \varphi_{1,0}, \cdots, \varphi_{R_0,0}, \beta_{1,0}, \cdots, \beta_{N_0,0}]^T$.

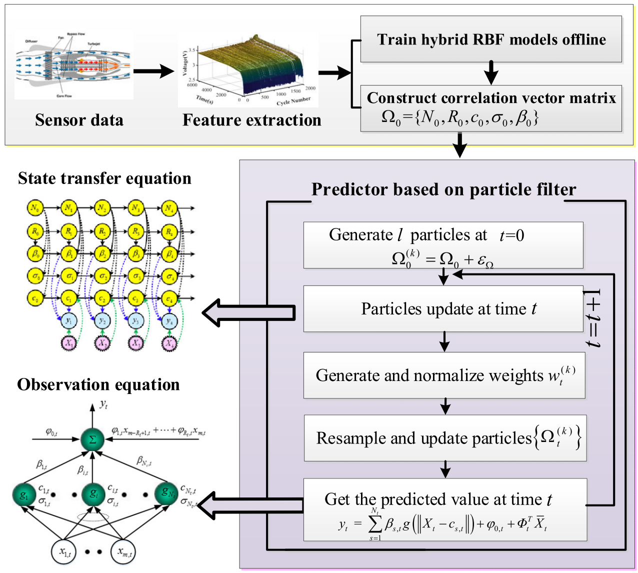

FIGURE 2. **Flow chart of variable structure hybrid RBF based on particle filter predictor.**

And then the initial state particle set $\left\{\Omega_0^{(k)}, w_0^{(k)}\right\}$ is established, where $\Omega_0^{(k)} = \Omega_0 + \varepsilon_\Omega$, $k = 1, 2, \cdots, l$, l is the number of particles, ε_Ω obey the standard normal distribution, and $w_0^{(k)}$ represents the particle weights.

Sampling according to the state transfer probability $p(\Omega_t^{(k)} | \Omega_{t-1}^{(k)})$, which according to the particle state transfer equation of Equation (5), the particle set $\left\{\tilde{\Omega}_t^{(k)}\right\}$ at time t is obtained, and $k = 1, 2, \cdots, l$.

The preliminary prediction value at time t can be obtained by using Equation (2) as the observation equation:

$$\hat{y}_{t|t-1}^{(k)} = f(\tilde{\Omega}_t^{(k)}) = H_t^{(k)} \beta_t^{(k)} \tag{11}$$

Assuming that the measured value at time t is y_t, then the importance weight update formula can be determined by combination of the likelihood function $p(y_t | \tilde{\Omega}_t^{(k)})$, state transfer probability $p(\tilde{\Omega}_t^{(k)} | \tilde{\Omega}_{t-1}^{(k)})$ and posterior probability $q(\tilde{\Omega}_t^{(k)} | \tilde{\Omega}_{t-1}^{(k)}, y_t)$ as follows:

$$\begin{aligned} \tilde{w}_t^{(k)} &\propto \tilde{w}_{t-1}^{(k)} \frac{p(y_t | \tilde{\Omega}_t^{(k)}) p(\tilde{\Omega}_t^{(k)} | \tilde{\Omega}_{t-1}^{(k)})}{q(\tilde{\Omega}_t^{(k)} | \tilde{\Omega}_{t-1}^{(k)}, y_t)} \\ &\propto \tilde{w}_{t-1}^{(k)} p(y_t | \tilde{\Omega}_t^{(k)}) \end{aligned} \tag{12}$$

wherein $q(\tilde{\Omega}_t^{(k)} | \tilde{\Omega}_{t-1}^{(k)}, y_t) = p(\tilde{\Omega}_t^{(k)} | \tilde{\Omega}_{t-1}^{(k)})$ as the function of particle importance density. In this study, based on the similarity measurement the particle weights are updated according to:

$$\tilde{w}_t^{(k)} = \frac{1}{\sqrt{2\pi\sigma^2}} \exp\left(-\frac{e_k^2}{2\sigma^2}\right) \tag{13}$$

wherein, σ represents the Gaussian distribution variance, e_k^2 represents the residual error between the initial estimated value $\hat{y}^{(k)}_{t|t-1}$ of the k particle and the measured value y_t. The weight after normalization is:

$$\bar{w}^{(k)}_t = \tilde{w}^{(k)}_t / \sum_{k=1}^{l} \tilde{w}^{(k)}_t \tag{14}$$

Then a new particle set $\left\{\Omega^{(k)}_t, {}^{1}/_{l}\right\}$ is established by using polynomial resampling method for resampling, which re-extracts l particles $\left\{\Omega^{(k)}_t\right\}$ from the particle set $\left\{\tilde{\Omega}^{(k)}_t, \bar{w}^{(k)}_t\right\}$.

The change of dimensionality of $c^{(k)}_{s,t}, \sigma^{(k)}_{s,t}, \beta^{(k)}_t$ are caused by the change of the parameters $N^{(k)}_t$, $R^{(k)}_t$ in particle $\left\{\Omega^{(k)}_t\right\}$, which in turn causes $H^{(k)}_t$, $\beta^{(k)}_t$ to change. Therefore, the parameter corresponding to the maximum weight is used to determine the final predicted value $\hat{y}_{t|t-1}$, namely:

$$\begin{cases} P_{\max} = \max pos\{\bar{w}^{(k)}_t, k = 1, 2, \cdots, l\} \\ \hat{y}_{t|t-1} = f(\Omega^{(P_{\max})}_t) = H^{(P_{\max})}_t \beta^{(P_{\max})}_t \end{cases} \tag{15}$$

wherein, $\max pos(\cdot)$ represents the function that takes the position of the maximum value in the set.

III. EGTM PREDICTION VERIFICATION BASED ON VARIABLE STRUCTURE HYBRID RBF NETWORK

A. EGTM DATA PREPROCESSING

In this study, the EGTM data obtained from 30 aero-engines of a certain type in an airline company from 1999 to 2008 [8] is selected for engine removal time prediction. Since the actual EGTM data of each engine obtained through EHM monitoring software is irregular data. In the selection of sample observation values, data preprocessing methods such as abnormal point analysis, noise processing and missing value supplementation [8] are adopted to preprocess the actual irregular EGTM data. The EGTM failure threshold of this type aero-engine is 30, and the sampling period is 200 flight cycles. Due to the different number of cycles before each engine failure, a total of 30 groups of EGTM data sets with different sample numbers were obtained, with totalling1564 EGTM data.

B. PREDICTIVE MODEL EVALUATION CRITERIA

To quantitatively measure and compare the prediction performance of the proposed methods, in this study the fixed structure RBF network model is also used for prediction in addition to the variable structure RBF model. By calculating the average absolute error (MAE), mean square error (MSE), and maximum error (MAX) between the predicted value of each algorithm and the true value of EGTM as the performance evaluation standard, the calculation formula is as shown in Equation (16)-(18) and use Equation (19) to calculate the 95% confidence interval (CI) of each algorithm's prediction result. $\overline{EGTM_{estimate}}$ and $cov(EGTM_{estimate})$ are mean value estimate and estimate covariance of EGTM.

$$E_{MAE} = \frac{1}{L}\sum_{i=1}^{L} \left|EGTM_{i,estimate} - EGTM_{i,real}\right| \tag{16}$$

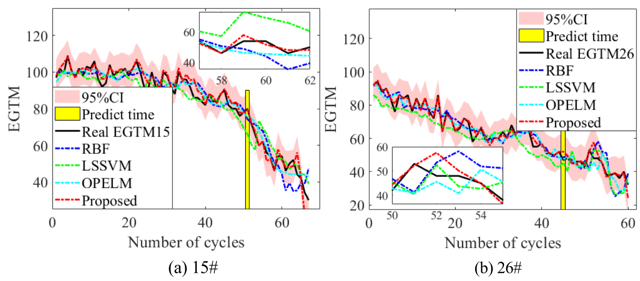

FIGURE 3. Forecast results based on EGTM data of a single engine.

$$E_{MSE} = \frac{1}{L}\sum_{i=1}^{L} \left(EGTM_{i,estimate} - EGTM_{i,real}\right)^2 \tag{17}$$

$$E_{MAX} = \max\left(\left|EGTM_{i,estimate} - EGTM_{i,real}\right|\right) \tag{18}$$

$$95\% confidencerangebounds \tag{19}$$

$$= \overline{EGTM_{estimate}} \mp 1.96 cov(EGTM_{estimate}) \tag{20}$$

C. EXPERIMENT AND RESULT ANALYSIS

The experiment is mainly divided into two parts—— experiment 1 uses the first 80% EGTM data of a single-engine as the training set, and the last 20% data as the test set for verification; experiment 2 uses the EGTM data of the first 24 engines to establish a prediction model. The data of the last 6 engines are used for test verification.

When establishing the fixed structure of RBF network, the trial-and-error method was adopted to initialize the number of hidden layer nodes N and the order of autoregressive model R, and the other parameters (i.e. the center vector C, the variance parameters σ, and the weight parameters β which composed of the connection weight between hidden layer nodes and output node of the RBF network and the coefficients of the autoregressive model) were mainly calculated by the self-organizing selection center learning method. For example, the 26 # engine in experiment 1, using the aforementioned method described, the structural parameters $N_0 = 20, R_0 = 5$, and the remaining 3 sets of parameters c_0, σ_0, and β_0 (parameter dimension is more, so they are not enumerated here) are obtained.

The adaptive-tunable-based hybrid RBF Network proposed in this paper for EGTM prediction, the initial value of network structure and parameters can be theoretically selected arbitrarily. However, for significantly restricting the search space of the structural parameters of the network, a set of initial parameters are obtained by pre-training the fixed structure of the hybrid RBF network. For example, the 26 # engine in experiment 1, the initial parameters of an adaptive-tunable-based hybrid RBF are consistent with those obtained by training fixed structure RBF, i.e., set $N_0 = 20, R_0 = 5, c_0, \sigma_0, \beta_0$, and as new samples are continuously added, the network structure and parameters can be adjusted dynamically, which can obtain a more accurate model structure and parameters in real-time.

TABLE 1. Error analysis of EGTM prediction results of 6 engines after experiment 2.

Engine number	Error type	Prediction method: RBF	LSSVM	OPELM	Proposed method
15#	E_{MSE}	89.65	54.97	41.76	**29.3060**
	E_{MAE}	8.26	6.37	5.16	**3.64**
	E_{MAX}	17.44	13.46	13.21	**13.12**
26#	E_{MSE}	78.43	63.62	38.68	**13.55**
	E_{MAE}	8.10	7.08	5.06	**2.27**
	E_{MAX}	13.87	12.95	11.92	**9.56**

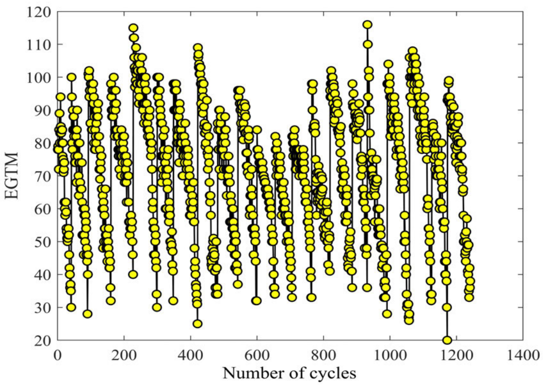

FIGURE 4. EGTM data of the first 24 engines.

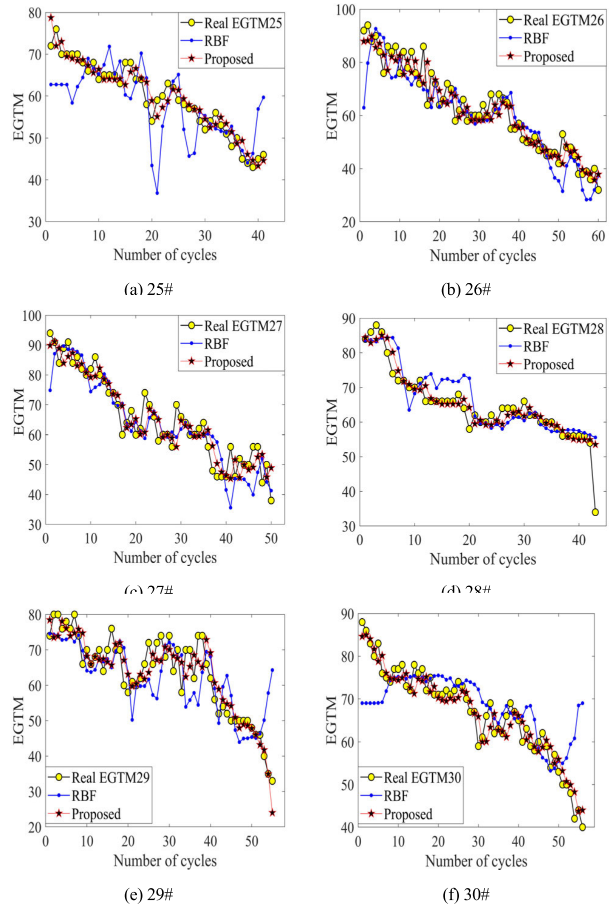

FIGURE 5. EGTM prediction results for the last 6 engines.

Accordingly, the EGTM prediction results of 2 engines (15# and 26#) randomly selected from the 30 engines provided in Experiment 1 are obtained, as shown in Figure 3. The other three algorithms, such as the fixed structure of RBF network, Least Squares Support Vector Machines (LSSVM) [22], and optimally-pruned extreme learning machine (OPELM) [23] are adopted as contrast models. Moreover, all algorithms in the experiments are selected optimum parameters.

From Figure 3, four methods can have good prediction performance on the EGTM data set for engines 15# and 26#, but it can be found the proposed prediction curve is closer to the real value by the local amplification figure. To quantitatively analyze the prediction performance, the numerical results of these four methods are presented in Table 1. It can be seen that the prediction MSE, MAE, MAX error of the proposed model has significantly lower. Due to the EGTM have strong nonlinear and time-varying characteristics, the fixed structure model cannot follow the EGTM variation process. However, the proposed method compared with the fixed structure based on RBF, LSSVM and OPELM algorithms has a more obvious advantage in prediction accuracy, the result is closer to the actual value.

Figure 4 presents all EGTM data for the first 24 engines described in Part A. Since the EGTM data of each engine is independent, the horizontal coordinate is set to represent the number of cycles, that is, the sample point, and the vertical coordinate is EGTM value. It can be seen from Figure 4 that the number of EGTM data obtained by each engine is different; however, the variation tendency is similar, which is helpful to dig out more dynamic characteristics or serviceable information of the EGTM data itself. Figure 5 shows the comparison results of the EGTM data of the last six engines based on the fixed structure RBF network model and the variable structure RBF model in this study, where the yellow circle is the actual engine EGTM data, the blue dot is the prediction result of the fixed structure RBF and the red star is the prediction result of the method proposed in this article. The results can be seen from Figure 5 that the method in this study has a better overall prediction effect than the fixed-structure RBF method.

Table 2 shows the accuracy results about the EGTM data of the last six engines under different methods. The results demonstrated that the proposed model possess a minor MSE, MAE and MAX error compared with the fixed-structure RBF. And the specific error reduction is shown in Table 3. The error obtained by fixed-structure RBF and the proposed method are denoted as A and B respectively, then the reduction is

TABLE 2. Error analysis of EGTM prediction results of 6 engines after experiment 2.

Method	Error type	Engine serial number 25#	26#	27#	28#	29#	30#
Fixed structure RBF	E_{MSE}	55.52	67.86	52.71	33.70	78.66	71.39
	E_{MAE}	5.82	6.22	5.45	3.95	6.59	5.81
	E_{MAX}	22.17	29.04	20.41	21.58	31.30	29.01
Method of this study	E_{MSE}	**7.58**	**29.94**	**27.82**	**14.77**	**23.39**	**9.75**
	E_{MAE}	**2.29**	**4.25**	**4.02**	**2.25**	**3.95**	**2.58**
	E_{MAX}	**6.74**	**16.15**	**13.97**	**19.55**	**10.29**	**6.85**

TABLE 3. Compared with the fixed structure RBF, the method in this paper reduces the percentage size (%).

Error type	Engine model 25#	26#	27#	28#	29#	30#
E_{MSE}	86.35	55.88	47.22	56.17	70.26	86.34
E_{MAE}	60.65	31.67	26.24	43.04	40.06	55.59
E_{MAX}	69.60	44.39	31.55	9.41	67.12	76.39

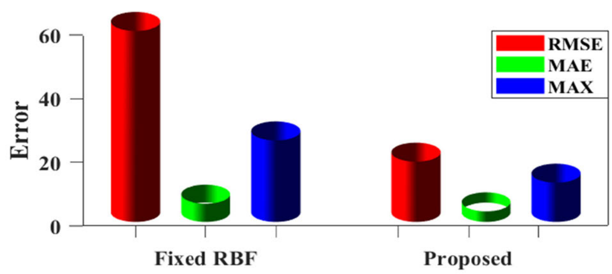

FIGURE 6. Average MSE, MAE, MAX error values predicted by EGTM for the last 6 engines.

calculated by $(A - B)/A$. From Table 3, it can be seen that the maximum reduction can be more than 80%. Comparing with the RBF, the average MSE, MAE, and MAX of the proposed model decreased by 67.04%, 42.88% and 49.75%, respectively. Overall, the prediction MSE, MAE, MAX error of the proposed model has significantly lower. The above results verify that the proposed model can effectively avoid the over-fitting phenomenon and accurately track the EGTM change process.

In order to more intuitive understanding on the results, the average MAE, RMSE, and MAX values obtained using two methods for the last six engines are given in Figure 6. Comparing with other method, the proposed model still has good estimation performance. Thus, these results illustrate the dynamic adjustment of the hybrid RBF network can improve the prediction accuracy and robustness.

The above experiments show that compared with the fixed structure RBF, the prediction results of the method proposed in this study are closer to the actual data, and the predictions of MSE, MAE, MAX error of the proposed model was significantly lower. The aforementioned experimental results substantiate that the dynamic adjustment of the hybrid RBF network can accurately capture the dynamic change information of EGTM in time, and further enhanced the prediction accuracy and robustness.

IV. CONCLUSION

To improve the prediction accuracy of aero-engine EGTM, a hybrid RBF neural network prediction model with a variable online structure is proposed. The core is to construct a hybrid RBF network composed of RBF network and linear regression terms to obtain the initial parameters of the model, and then a Brownian motion with drift and scale coefficients and particle filter are adopted to dynamically adjust the hybrid RBF network structure and parameters. The experimental results demonstrate that compared with the fixed structure RBF, the prediction accuracy of the method proposed in this study is significantly improved, and the three error indicators (MSE, MAE, MAX) declined dramatically, average MSE, MAE, and MAX errors decreased by 67.04%, 42.88% and 49.75%, respectively, when predicting the EGTM of six different engines. And the results illustrate that the proposed adaptive-tunable-based hybrid RBF network can capture the dynamic nature of EGTM in time during the forecasting process.

In addition, due to the high robustness of the hybrid RBF model with the variable online structure proposed in this study, the algorithm can also be applied to predict other performance parameters of aero-engines under different working conditions, such as engine speed, oil consumption, etc. Besides, it is worth mentioning that complex neural network structures such as LSTM can also be selected, and then real-time dynamic adjustment of LSTM structure can be carried out by using the ideas in this paper, which can be taken as the future work. Theoretically, the posterior estimate described by the state probability distribution will be equal to the true value only as the selected particle data approaches infinity. However, the number of particles in this study is fixed, how to select the appropriate number of particles and how to design a more effective resampling algorithm will be the focus of the next research to improve the prediction accuracy of EGTM.

REFERENCES

[1] D. Dimogianopoulos, J. Hios, and S. Fassois, "Aircraft engine health management via stochastic modelling of flight data interrelations," *Aerosp. Sci. Technol.*, vol. 16, no. 1, pp. 70–81, Jan. 2012.
[2] K. Peng, R. Jiao, J. Dong, and Y. Pi, "A deep belief network based health indicator construction and remaining useful life prediction using improved particle filter," *Neurocomputing*, vol. 361, pp. 19–28, Oct. 2019.
[3] D. Miljkovic, "Detecting aircraft piston engine problems by analysis of engine parameters," in *Proc. 42nd Int. Conv. Inf. Commun. Technol., Electron. Microelectron. (MIPRO)*, May 2019, pp. 937–942.
[4] D. Chen and J. Sun, "Fuel and emission reduction assessment for civil aircraft engine fleet on-wing washing," *Transp. Res. D, Transp. Environ.*, vol. 65, pp. 324–331, Dec. 2018.
[5] M. T. Yildirim and B. Kurt, "Aircraft gas turbine engine health monitoring system by real flight data," *Int. J. Aerosp. Eng.*, vol. 2018, Mar. 2018, Art. no. 9570873.

[6] W. Peng, Z.-S. Ye, and N. Chen, "Bayesian deep-learning-based health prognostics toward prognostics uncertainty," *IEEE Trans. Ind. Electron.*, vol. 67, no. 3, pp. 2283–2293, Mar. 2020.
[7] A. Kumar, A. Srivastava, N. Goel, and J. Mcmaster, "Exhaust gas temperature data prediction by autoregressive models," in *Proc. IEEE 28th Can. Conf. Electr. Comput. Eng. (CCECE)*, Halifax, Canada, May 2015, pp. 976–981.
[8] S. H. Ren, "Research on methods of performance reliability assessments and life on wing prediction for civil aeroengine," Nanjing Univ. Aeronaut. Astronaut., Nanjing, China, 2010.
[9] Y. Gao and N. Wang, "Aero-engine condition monitoring based on Kalman filter theory," *Adv. Mater. Res.*, vol. 490, pp. 176–181, Feb. 2012.
[10] M. Ilbas and M. Turkmen, "Estimation of exhaust gas temperature using artificial neural network in turbofan engines," *J. Thermal Sci. Technol.*, vol. 32, no. 2, pp. 11–18, 2012.
[11] I. Koleini, A. Roudbari, and V. Marefat, "EGT prediction of a micro gas turbine using statistical and artificial intelligence approach," *IEEE Aerosp. Electron. Syst. Mag.*, vol. 33, no. 7, pp. 4–13, Jul. 2018.
[12] A. A. Rai, P. S. Pai, and B. R. S. Rao, "Prediction models for performance and emissions of a dual fuel CI engine using ANFIS," *Sadhana*, vol. 40, no. 2, pp. 515–535, Apr. 2015.
[13] H. F. Yang and X. L. Jia, "Aero engine exhaust gas temperature prediction based on LSTM," *Aviation Comput. Technol.*, vol. 48, no. 04, pp. 61–65, 2018.
[14] C.-G. Huang, H.-Z. Huang, and Y.-F. Li, "A bidirectional LSTM prognostics method under multiple operational conditions," *IEEE Trans. Ind. Electron.*, vol. 66, no. 11, pp. 8792–8802, Nov. 2019.
[15] J. Pi, S. Ma, and Q. Zhang, "Aero-engine exhaust gas temperature prediction model based on IFOA-GRNN," *Aerodynamics*, vol. 66, no. 11, pp. 8792–8802, 2019.
[16] G. Mao, C. Zhang, K. Shi, and P. Wang, "Prediction of the performance and exhaust emissions of ethanol-diesel engine using different neural network," *Energy Sour., A, Recovery, Utilization, Environ. Effects*, vol. 4, pp. 1–15, Aug. 2019.
[17] X. Zeng, H. Peng, and F. Zhou, "A regularized SNPOM for stable parameter estimation of RBF-AR(X) model," *IEEE Trans. Neural Netw. Learn. Syst.*, vol. 29, no. 4, pp. 779–791, Apr. 2018.
[18] Y. Xiao and D. Pan, "Research on scale adaptive particle filter tracker with feature integration," *Int. J. Speech Technol.*, vol. 49, no. 11, pp. 3864–3880, Nov. 2019.
[19] D. Wang and K.-L. Tsui, "Brownian motion with adaptive drift for remaining useful life prediction: Revisited," *Mech. Syst. Signal Process.*, vol. 99, pp. 691–701, Jan. 2018.
[20] T. Similä and J. Tikka, *Multiresponse Sparse Regression With Application to Multidimensional Scaling*. Berlin, Germany: Springer, 2005, pp. 97–102.
[21] P. Coulibaly and N. D. Evora, "Comparison of neural network methods for infilling missing daily weather records," *J. Hydrol.*, vol. 341, nos. 1–2, pp. 27–41, Jul. 2007.
[22] J. A. K. Suykens, T. V. Gestel, J. D. Brabanter, B. D. Moor, and J. Vandewalle, "Least squares support vector machines," *Int. J. Circuit Theory Appl.*, vol. 27, no. 6, pp. 605–615, 2002.
[23] Z. Liu, W. Mei, X. Zeng, C. Yang, and X. Zhou, "Remaining useful life estimation of insulated gate biploar transistors (IGBTs) based on a novel volterra k-Nearest neighbor optimally pruned extreme learning machine (VKOPP) model using degradation data," *Sensors*, vol. 17, no. 11, p. 2524, Nov. 2017.

YUAN LIU was born in Jingjiang, Jiangsu, China, in 1991. He received the B.S. and M.S. degrees in aerospace propulsion theory and engineering from the Nanjing University of Aeronautics and Astronautics, in 2013 and 2016, respectively. Since 2016, he has been an Aeroengine Engineer with the AECC Hunan Aviation Powerplant Research Institute, Zhuzhou, China. He is the author of more than 15 articles and holds more than five inventions. His interests include overall performance design of aeroengine, fault diagnosis of aeroengine, aeroengine automatic control, and aeroengine health management.

XIANPING ZENG received the M.S. degree in instrument science and technology from the University of Electronic Science and Technology of China, Chengdu, China, in 2016. She is currently pursuing the Ph.D. degree in measurement technology and instruments with Xiamen University, Xiamen, China. Her research interests include pattern recognition, aircraft health management, and structural health monitoring.

YANYUN TIAN was born in Zhuzhou, Hunan, China, in 1991. She received the M.S. degree in aerospace propulsion theory and engineering from the Nanjing University of Aeronautics and Astronautics, in 2013. Since 2016, she has been an Aeroengine Engineer with the Hunan Institute of Power Machinery, AVIC, Zhuzhou. Her main research interests include aeroengine automatic control and aeroengine health management.

YISHOU WANG received the B.Sc. and Ph.D. degrees from the Dalian University of Technology, Dalian, China, in 2002 and 2008, respectively. He is currently an Associate Professor with Xiamen University, Xiamen, China. His main research interests include engine health management, structural health monitoring, and advanced sensing technology.

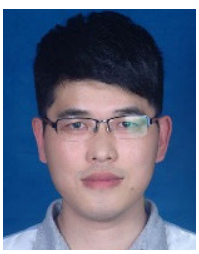

HANLIN SHENG (Member, IEEE) received the B.S. degree in flight vehicle propulsion engineering and the Ph.D. degree in aerospace propulsion theory and engineering from the Nanjing University of Aeronautics and Astronautics, Nanjing, China, in 2009 and 2015, respectively. From 2015 to 2016, he was a Postdoctoral Fellow with Nanyang Technological University. He is currently an Assistant Professor with the School of Energy and Power Engineering, Nanjing University of Aeronautics and Astronautics. His research interest includes aircraft and aeroengine modeling, simulation, and control.